Journal of the European Ceramic Society **6** (1990) 111-117

Structure and Ionic Conductivity of Solid Solutions in the System $0{\cdot}9\{(ZrO_2)_{1-x}-(CeO_2)_x\}-0{\cdot}1(Y_2O_3)$

P. V. Ananthapadmanabhan,[a] N. Venkatramani,[a] V. K. Rohatgi,[a] A. C. Momin[b] & K. S. Venkateswarlu[b]

[a] Plasma Physics Division, [b] Water Chemistry Division, Bhabha Atomic Research Centre, Bombay 400085, India

(Received 26 July 1989; revised version received 16 February 1990; accepted 21 February 1990)

Abstract

Solid solutions in the ternary system ZrO_2–CeO_2–Y_2O_3, by virtue of their high-temperature stability and good electrical conductivity, have potential application in many advanced technologies such as the magnetohydrodynamic (MHD) generator. The investigations reported here include studies on the structure, electrical conductivity and oxygen ion transport number of solid solutions in the system $0{\cdot}9\{(ZrO_2)_{1-x}-(CeO_2)_x\}-0{\cdot}1(Y_2O_3)$ in the temperature range 1000–1600 K in static air. It is found that electrical conduction proceeds by transport of oxygen ions through the network of oxygen vacancies in the lattice. The variation of conductivity with composition has been analysed in relation to the changes in lattice parameter and scattering of oxygen ions.

Mischkristallzusammensetzungen im Dreistoffsystem ZrO_2–CeO_2–Y_2O_3 besitzen wegen ihrer Stabilität bei hoher Temperatur und ihrer guten elektrischen Leitfähigkeit in vielen fortschrittlichen Technologien wie dem magnetohydrodynamischen Generator (MHD) mögliche Anwendungsgebiete. Die hier aufgeführten Untersuchungen schließen Studien der Struktur, der elektrischen Leitfähigkeit und der Transportzahl der Sauerstoffionen von Mischkristallzusammensetzungen im System $0{\cdot}9((ZrO_2)_{1-x}-(CeO_2)_x)-0{\cdot}1Y_2O_3$ im Temperaturbereich 1000–1600 K in stehender Luft ein. Die elektrische Leitfähigkeit gründet sich auf den Transport von Sauerstoffionen durch die Sauerstoffleerstellen im Atomgitter. Die Abhängigkeit der Leitfähigkeit von der Zusammensetzung wurde mit der Änderung der Gitterparameter und der Streuung der Sauerstoffionen in Bezug gesetzt.

En raison de leur stabilité à haute température et de leur bonne conductivité électrique, les solutions solides du système ternaire ZrO_2–CeO_2–Y_2O_3 trouvent de nombreuses applications dans diverses techniques de pointe, comme celle du générateur magnétohydrodynamique (MHD) par exemple. On a étudié ici la structure, la conductivité électrique et le nombre de transport de l'ion oxygène de solutions solides du système $0{\cdot}9\{(ZrO_2)_{1-x}-(CeO_2)_x\}-0{\cdot}1(Y_2O_3)$ à des températures comprises entre 1000 et 1600 K sous atmosphère stagnante d'air. On a trouvé que la conduction électrique est due au transport d'ions oxygène à travers les lacunes du réseau cristallin. On a expliqué les variations de conductivité en fonction de la composition par la modification du paramètre de maille et la distribution des ions oxygène.

1 Introduction

Zirconia-based materials find potential application in many advanced technologies such as the magnetohydrodynamic (MHD) generator, high-temperature fuel cells, etc.[1,2] Calcia-stabilised zirconia (CSZ) and yttria-stabilised zirconia (YSZ) have been extensively studied for application as electrodes in MHD channels. The general mechanism of electrical conduction in these materials is by the migration of oxygen vacancies, and this ionic nature of conductivity is a serious limitation.[3]

Incorporation of ceria has been attempted to circumvent this problem. The expectation was that cerium, being a transition metal, could change its valency at high temperatures and low oxygen partial pressures, to give enhanced conductivity. Results of investigations on the electrical properties of the binary system ZrO_2–CeO_2 show that the high-ceria

Journal of the European Ceramic Society 0955-2219/90/$3.50

cubic solid solution has good electrical conductivity, electrons being the predominant charge carriers.[4] The mode of conduction is by 'hopping' of electrons between Ce^{4+} and Ce^{3+} sites. However, the preferential volatilisation of CeO_2 at higher temperatures is a drawback. Attempts to combine the desirable features of YSZ and the CeO_2–ZrO_2 system have led to the study of the ternary system ZrO_2–CeO_2–Y_2O_3. The ternary system $0{\cdot}9\{(ZrO_2)_{1-x}$–$(CeO_2)_x\}$–$0{\cdot}1(Y_2O_3)$ has a cubic structure throughout its composition range. The presence of yttria, besides ensuring a cubic symmetry, improves the thermal stability of the material.

2 Theoretical aspects

The addition of a trivalent oxide such as Y_2O_3 to pure CeO_2 or ZrO_2 results in oxygen vacancies in the crystal structure according to the following equation:

$$Y_2O_3 \rightarrow 2Y'_{Zr} + 3O_O^x + V_O^{\cdot\cdot} \quad (1)$$

In terms of the Kroger–Vink notation,[5] which will be used throughout this paper, Y'_{Zr} represents an yttrium atom with an effective charge of -1 in the zirconium sublattice, O_O^x a neutral oxygen atom and $V_O^{\cdot\cdot}$ an oxygen vacancy with a double positive charge. The following equilibrium with its surrounding atmosphere is always implied inside the crystal:

$$O_O^x \rightarrow V_O^{\cdot\cdot} + 2e + \tfrac{1}{2}O_2(g) \quad (2)$$

Applying the law of mass action to this equilibrium, the equilibrium constant can be expressed in terms of concentration of oxygen vacancies, electrons and oxygen partial pressure:

$$C_1 = [V_O^{\cdot\cdot}]n^2p^{1/2} \quad (3)$$

where $[V_O^{\cdot\cdot}]$ and n represent the concentrations of oxygen vacancies and electrons respectively and p the equilibrium oxygen partial pressure. The solution is assumed to be dilute so that the concentration of neutral oxygen atoms essentially remains constant and does not enter the equation.

In the ternary system ZrO_2–CeO_2–Y_2O_3, apart from the oxygen vacancies created by the partial replacement of Zr^{4+} or Ce^{4+} by Y^{3+} ions, loss of oxygen from CeO_2 at high temperatures and in reducing atmospheres also generates oxygen vacancies:

$$CeO_2 \rightarrow \tfrac{1}{2}Ce_2O_3 + \tfrac{1}{2}O_2 \quad (4)$$

The above equation is biased to the right above 1700 K even in the presence of oxygen and when in solid solution with ZrO_2.[6] The redox reaction can also be represented as

$$2Ce_{Ce}^x + 4O_O^x = 2Ce'_{Ce} + 3O_O^x + V_O^{\cdot\cdot} + \tfrac{1}{2}O_2(g) \quad (5)$$

The electrons released in the reduction process are localised in cerium sites, which become reduced to Ce^{3+} and are represented as Ce'_{Ce}. The electrical conductivity is enhanced considerably and proceeds by hopping of the electrons between Ce^{4+} and Ce^{3+} sites. Assuming that the deviation from stoichiometry is small, the equilibrium constant for the above redox reaction can be written as

$$C_2 = [V_O^{\cdot\cdot}][Ce']^2p^{1/2} \quad (6)$$

It may be seen from (5) that for every one oxygen vacancy created two Ce′ are generated. In other words,

$$[V_O^{\cdot\cdot}] = 2[Ce'_{Ce}] \quad (7)$$

Expressing $[V_O^{\cdot\cdot}]$ in terms of $[Ce']$ and substituting in equation (6), we obtain

$$C_3 = [Ce'_{Ce}]^3p^{1/2} \quad (8)$$

From (8) it is clear that $[Ce'_{Ce}]$, and hence σ (the electrical conductivity of the solid solution), is proportional to $p^{-1/6}$. However, for the ternary system under consideration, this situation arises only at higher temperatures and lower oxygen partial pressures. The variation of electrical conductivity with oxygen partial pressure has been investigated by Cales and Baumard,[7] and the present study is restricted to the ionic region only.

3 Sample Preparation and Electrical Conductivity Measurements

High-purity powders (−325 mesh) of CeO_2, Y_2O_3 and ZrO_2 (containing 2·4% HfO_2), supplied by M/s. Indian Rare Earths Ltd, were used as the starting materials. The presence of HfO_2 in ZrO_2 should not affect the results to any significant extent, as the physical properties of ZrO_2 and HfO_2 are very similar.[8] Solid solutions of $0{\cdot}9\{(ZrO_2)_{1-x}$–$(CeO_2)_x\}$–$0{\cdot}1(Y_2O_3)$ were prepared, covering the entire range from $x=0$ to $x=1$ in steps of 0·1. Sintered specimens of the solid solutions were prepared by the conventional powder metallurgical technique. This consisted in mixing the component oxides in appropriate amounts to give the required compositions and grinding in a planetary ball mill. To ensure thorough mixing of the powders, a suitable quantity of acetone was added during the mixing operation. The powder mixture was then dried and compacted into discs of 25-mm diameter and 3–5-mm thickness by uniaxial pressing at

60 MPa. About 0·5% polyethylene glycol was added to serve as binder. The pellets were then fired at 1673 K for 3 h. The prefired pellets were crushed, ground to a fine powder, compacted at 90 MPa and sintered at 1873 K for 16 h. The porosity of the sintered pellets did not exceed 10%.

The sintered materials were then subjected to X-ray powder diffraction to check the completeness of the reaction. The specimens were crushed to a fineness of −200 mesh and the diffraction patterns were recorded using Ni-filtered Cu K_α radiation. All compositions, over the entire range, showed a single homogeneous phase which had the fluorite structure.

Electrical conductivity was measured by the DC four-probe technique on sintered circular samples of 25-mm diameter and 3–5-mm thickness, up to 1673 K in static air. The sample temperature was monitored by a Pt–Pt–13% Rh thermocouple located in the vicinity of the sample. Conductivity measurements were taken at temperature intervals of 100 K. Current and voltage readings were taken only after the sample attained thermal equilibrium.

To determine the ionic contribution to the electrical conductivity, the oxygen ion transport number was measured by the electrochemical method. This consisted in setting up an oxygen concentration cell by maintaining a gradient of oxygen potential across the sintered specimen and measuring the emf of the cell at various temperatures. Construction details of the experimental set-up have been described elsewhere.[9] The oxygen transport number was calculated by using the following equation:

$$E = 2{\cdot}303 t_{\text{ion}} \frac{RT}{NF} \log \frac{p_1}{p_2} \qquad (9)$$

where E is the open circuit voltage of the cell, R is the universal gas constant, F is the Faraday constant, and p_1 and p_2 are the partial pressures of oxygen on the inner and outer sides of the sample.

However, for better accuracy, the emf value of each sample at a particular temperature and oxygen potential gradient was compared with the corresponding emf value of an yttria-stabilised zirconia standard cell which has $t_{\text{ion}} = 1$ over a wide ranges of temperature and oxygen pressure. The ratio E/E^0, where E and E^0 are the emf of the sample and the standard cell respectively, gave the value of t_{ion}.

4 Results and Discussion

X-Ray powder diffraction analysis indicates a homogeneous single-phase solid solution which has

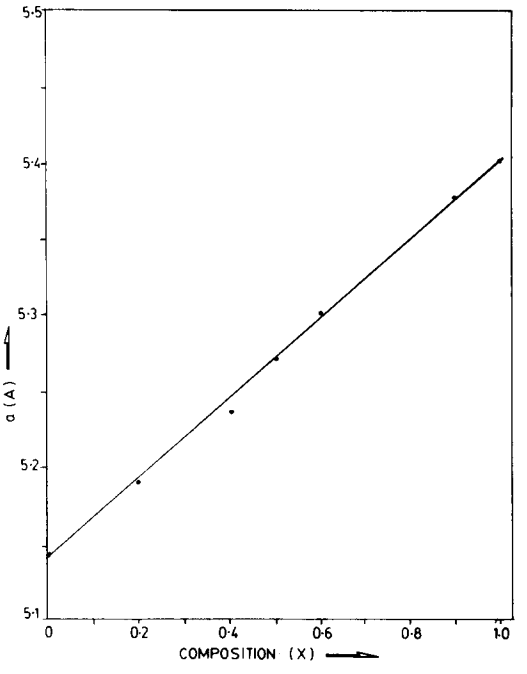

Fig. 1. Variation of lattice parameter (a) with composition (x) in the ternary system 0·9{ZrO_2–CeO_2}–0·1Y_2O_3.

the fluorite structure for all compositions in the system. The values of the lattice parameter for the end-members in the system, i.e. for $x = 0$ and $x = 1$, agree reasonably well with those reported earlier.[7] The variation of the lattice parameter a with x, where x is the composition expressed in terms of the fraction (molar) of ZrO_2 replaced by CeO_2, shows linear behaviour (see Fig. 1). This variation can be expressed by

$$a = 5{\cdot}1358 + 0{\cdot}2642x \qquad (10)$$

Theoretical density was evaluated from the values of the cell constant. Values of the theoretical density calculated for the oxygen vacancy model are in good agreement with the pycnometric densities, and indicate the substitutional nature of the solid solutions and the presence of oxygen vacancies as the predominant defects.

The variation of electrical conductivity with temperature is shown in Fig. 2, where $\log \sigma$ is plotted against reciprocal temperature. The linear nature of the graphs in all cases suggests that the dependence of conductivity on temperature can be expressed by the following equation:

$$\sigma = \sigma_0 \exp(-E_a/kT) \qquad (11)$$

where E_a represents the activation energy, k is Boltzman's constant and T is the absolute temperature. The activation energy was determined from the slope of $\log \sigma$ vs $1/T$ curve.

The isothermal variation of electrical conductivity as a function of x, the ratio of the fraction of ZrO_2

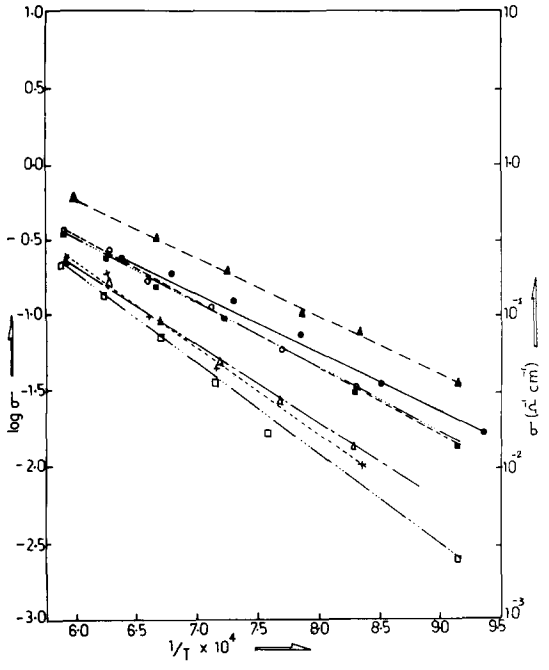

Fig. 2. Variation of $\log \sigma$ with $1/T$ for solid solutions in the ternary system $0{\cdot}9\{ZrO_2$–$CeO_2\}$–$0{\cdot}1Y_2O_3$. ●, $x = 0{\cdot}0$; ■, 0·1; △, 0·4; □, 0·5; ×, 0·6; ○, 0·9; ▲, 1·0.

replaced by CeO_2, is depicted in Fig. 3. The conductivity first increases with x, reaching a minimum at $x = 0{\cdot}5$, and then increases again. In other words, incorporation of CeO_2 in $0{\cdot}9ZrO_2$–$0{\cdot}1Y_2O_3$ or ZrO_2 in $0{\cdot}9CeO_2$–$0{\cdot}1Y_2O_3$ results in a decrease in conductivity. This behaviour holds good at all temperatures at which measurements were made in this study. However, at higher temperatures the dip in the curve decreases, i.e. the curves tend to flatten at higher temperatures. The variation of activation energy, on the other hand, follows the reverse trend. This is shown in Fig. 4. Activation

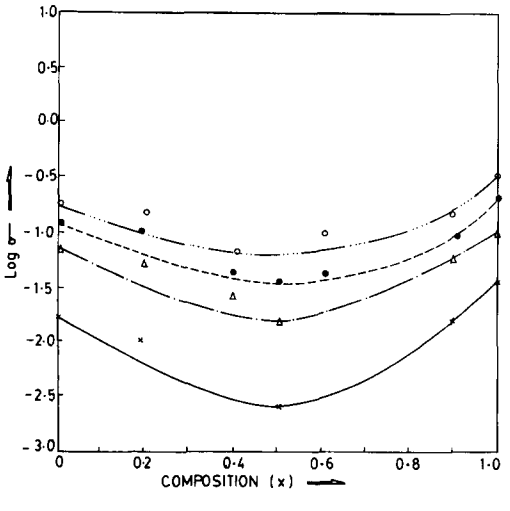

Fig. 3. Variation of $\log \sigma$ (isothermal) with composition (x). ○, ——·——, 1471K; ●, – – – –, 1373K; △, —·—·—, 1300K; ×, ———, 1073K.

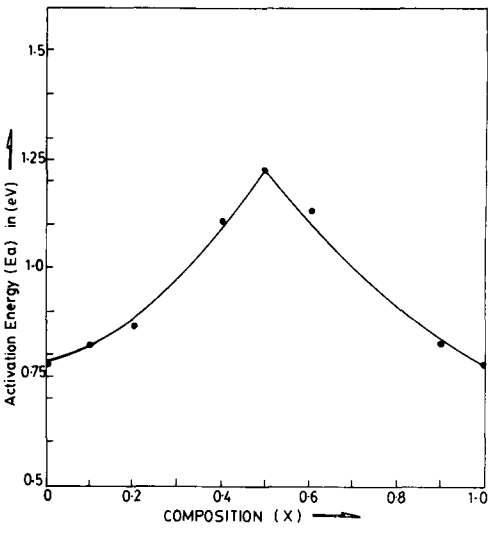

Fig. 4. Variation of activation energy with composition (x).

energy increases from 0·76 eV for the composition $0{\cdot}9ZrO_2$–$0{\cdot}1Y_2O_3$, reaches a maximum of 1·23 eV for $x = 0{\cdot}5$, which corresponds to the composition $0{\cdot}45ZrO_2$–$0{\cdot}45CeO_2$–$0{\cdot}1Y_2O_3$, and falls off to 0·78 eV for the composition $0{\cdot}9CeO_2$–$0{\cdot}1Y_2O_3$. This also explains why the dip in the $\log \sigma$ versus x curve decreases with temperature (i.e. the flattening of the curves at higher temperatures).

Results of oxygen ion transport measurements are shown in Fig. 5, where the cell emf is plotted as a function of the absolute temperature. As the ratio of the oxygen partial pressures on either side of the

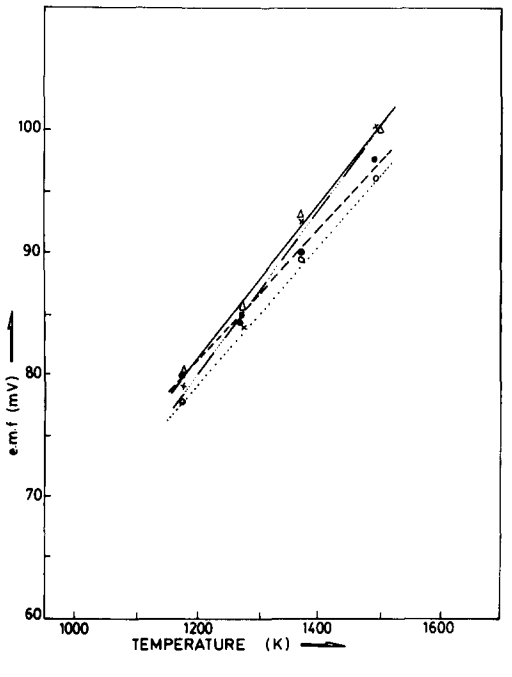

Fig. 5. Variation of EMF with temperature (K) for the standard and the samples. ———, $0{\cdot}9ZrO_2$–$0{\cdot}1Y_2O_3$ (standard); – – –, $0{\cdot}45CeO_2$–$0{\cdot}45ZrO_2$–$0{\cdot}1Y_2O_3$; ——·——, $0{\cdot}9CeO_2$–$0{\cdot}1Y_2O_3$; ····, $0{\cdot}54CeO_2$–$0{\cdot}36ZrO_2$–$0{\cdot}1Y_2O_3$.

sample, p_1/p_2, remains constant for all temperatures, equation (9) can be rewritten as

$$E = C' t_{ion}\, T \qquad (12)$$

where C' is a constant involving R, F and $\log p_1/p_2$. Thus E is a function only of temperature and t_{ion}. It is, therefore, evident from the linear nature of the E versus T curves that t_{ion} remains constant up to 1600 K. Further, $t_{ion} = E/E^0$ remains essentially close to unity, showing thereby that oxygen ions are the predominant current-carrying species. However, in the case of high-ceria compositions, deviation from linearity in the E versus T curve is noticeable above 1500 K, indicating the onset of electronic conduction.

The above findings suggest that partial replacement of ZrO_2 by CeO_2 in the binary solid solution $0{\cdot}9ZrO_2$–$0{\cdot}1Y_2O_3$ results in increasing the hindrance to the motion of oxygen ions. The same is true for the binary composition $0{\cdot}9CeO_2$–$0{\cdot}1Y_2O_3$. As the concentration of oxygen vacancies, $[V_O^{\cdot\cdot}]$, remains constant for all the compositions (except for a negligible decrease due to a slight increase in the lattice volume), the observed nature of conductivity change with composition is rather surprising. This also indicates that the variation in conductivity is a consequence of the change in mobility of the oxygen ions with composition. In fact, the mobility versus x curve should be similar to the $\log\sigma$ versus x curve. This strongly indicates that the mobility of the migrating oxygen ions is influenced by changes in lattice parameter, effective cation radius and the nature of the cations.

5 Structure and Electrical Conductivity

A description of the fluorite structure, to which all the compositions in this system belong, will not be out of place in this context. The crystal structure of a typical MO_2–R_2O_3 solid solution crystallising in the fluorite structure is shown in Fig. 6(a). A better understanding of the arrangement of atoms in the unit cell can be had by dividing the unit cell into eight equivalent cubelets by bisecting the edges of the unit cell. One such cubelet is shown in Fig. 6(b), with an oxide ion at the body centre and the cations arranged in tetrahedral co-ordination about the oxide ion. If any electronic contribution to electrical conductivity is neglected, then conduction results by the migration of oxygen ions (migration of oxygen vacancies in the opposite direction) through channels formed by the neighbouring cations under the influence of an applied electric field. Obviously,

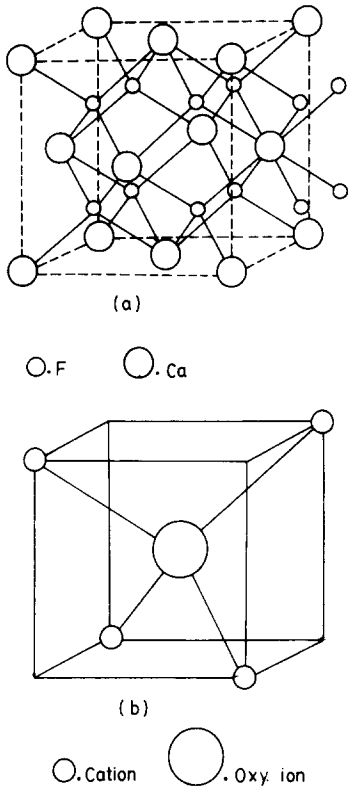

Fig. 6. (a) Typical fluorite structure. (b) Schematic representation of oxygen coordination in fluorite structure.

the larger the channel radius the more mobile the oxygen ions, and consequently the greater the conductivity. Also, the activation energy is reduced. The radius of this channel, s, is related to the lattice parameter, a, and the average cation radius, r_c, by the following equation:[10]

$$s = a/\sqrt{6} - \bar{r}_c \qquad (13)$$

It can be seen from (13) that the channel radius increases with the lattice parameter and hence with x, and the electrical conductivity is expected to increase with x.

The difference between the metal(cation)–oxygen distance, r, and the sum of the radii[11] of the cation and anion ($d = r - \{r^+ + r^-\}$) gives a measure of the 'tightness' of the bond. For the fluorite structure, d is related to the cell parameter by the equation

$$d = a\sqrt{3}/4 - (r^+ + r^-) \qquad (14)$$

On the basis of this parameter, the conductivity also is expected to increase with the composition. The failure of these parameters to explain the experimentally observed variation of conductivity is the result of some tacit assumptions involved in the discussion. We have neglected the influence of composition on the mobility and scattering of the oxygen ions. In fact, the experimental results suggest that the scattering of the oxygen vacancies is affected

to a significantly greater extent so as to offset the effect of the increase in channel radius. The following simple model attempts to correlate the variation of conductivity with composition on the basis of scattering of oxygen ions.

6 Model

Let the cations be arranged in parallel rows, the distance of separation between the cations being determined by the lattice parameter, anion radius, bond strength, etc. As the concentration of Y_2O_3 is constant (10 mol%) throughout, and as the replacement of Zr^{4+} by Ce^{4+} or vice versa does not involve any valence change, it is assumed that the binary solid solution $0{\cdot}9ZrO_2$–$0{\cdot}1Y_2O_3$ can be represented by MO_{2-v}, where M is a hypothetical cation with an effective valency (between three and four) and effective radius and v is the number of oxygen vacancies per molecule. The oxide ions are arranged between the rows of cations, the cation–anion distance being determined by the minimum energy criterion. Similarly, we let $M'O_{2-v}$ represent $0{\cdot}9CeO_2$–$0{\cdot}1Y_2O_3$. Electrical conductivity results from the motion of oxygen ions through the network of oxygen vacancies when an electric field is applied.

In the case of MO_{2-v} or $M'O_{2-v}$, the oxygen ions and vacancies are situated at points equidistant from the top and bottom rows of cations. Thus the motion of the oxygen ions, under the influence of an electric field, is along a straight-line path. However, when we consider any other composition where some of the M ions have been replaced by M′ ions of different radius, the straight-line path of the oxygen ions is disturbed because of increased scattering of the oxygen ions. This is because the lattice parameter does not vary to the same extent as the effective cation radius. This is evident from Fig. 7, which shows that although the effective cation radius increases by ~13% on going from MO_{2-v} to $M'O_{2-v}$, the increase in lattice constant is only 5%. This causes scattering of the oxygen ions, and the degree of scattering reaches a maximum at [M]/[M′] = 1. This argument holds equally good when we start from $M'O_{2-v}$, progressively replacing M′ by M. Further replacement of M by M′ (or M′ by M) again reduces the scattering. This suggests that the oxygen path length (the actual path taken by the migrating oxygen ions) is a function of the fraction of sites occupied by M as well as M′. In other words,

$$l = Kx(1-x) \tag{15}$$

where l is the oxygen path length, x is the mol fraction of MO_{2-v}, $1-x$ is the mol fraction of $M'O_{2-v}$ and K is a constant which has the dimension of length.

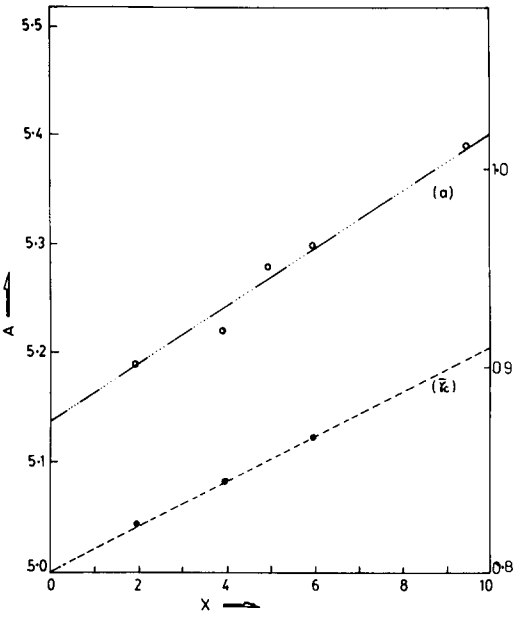

Fig. 7. Variation of cell parameter (a) and effective cation radius ($\bar{r}_c$) with composition (x).

The variation of this function with x is similar to that of the activation energy with x, which indicates the appropriateness of the choice of the function. Differentiation of equation (15) with respect to x gives

$$dl/dx = K(1-2x) \tag{16}$$

Equation (16) on further differentiation yields

$$d^2l/dx^2 = -2K \tag{17}$$

When l is maximum, $dl/dx = 0 = K(1-2x)$, the solution of which gives $x = 0{\cdot}5$. As l is inversely proportional to conductivity, a maximum path length would mean minimum conductivity. Thus the model predicts that the conductivity is minimum at $x = 0{\cdot}5$, corresponding to the composition $0{\cdot}45ZrO_2$–$0{\cdot}45CeO_2$–$0{\cdot}1Y_2O_3$, or in line with the experimental observation.

According to the above model, the progressive replacement of ZrO_2 by CeO_2 in $0{\cdot}9ZrO_2$–$0{\cdot}1Y_2O_3$, or that of CeO_2 by ZrO_2 in $0{\cdot}9CeO_2$–$0{\cdot}1Y_2O_3$, results in increased impedence to the motion of charge carriers, despite the fact that the charge carrier density remains constant. This increased hindrance to the oxygen mobility is because of the increased scattering of oxygen ions; the extent of this scattering reaches a maximum when Zr and Ce are present in equimolar quantities, corresponding to the composition $0{\cdot}45ZrO_2$–$0{\cdot}45CeO_2$–$0{\cdot}1Y_2O_3$. It

may be noted that at this composition the probability of Zr^{4+} and Ce^{4+} being juxtaposed is maximum, which means that the frequency of oxygen ions encountering unlike cations is maximum. As a consequence of this, the oxygen path is distorted to the maximum extent and the conductivity is minimum.

This situation is similar to that observed in alloy systems, where alloying of a pure metal leads to enhanced electrical resistance.[12] Local inhomogeneities in the crystal structure produced by the differences in the size of the different atoms cause increased scattering of the electrons, particularly in solid solution alloys, which results in lowering of conductivity. In the unannealed or random solid solution, resistivity attains a maximum at the 50–50 composition, as this corresponds to the maximum possible distortion of the structure, and drops rapidly at both ends as the pure metals are approached.

In the light of the above arguments, the extent of scattering of the oxygen ions is reflected in terms of changes in the path length, l. It is seen from equation (15) that $l=0$ for $x=0$ and $x=1$. In other words, the extent of scattering is at a minimum at the two extreme binary compositions, because the inhomogeneities in the ionic radii are reduced to the minimum as the end binary compositions are approached, which results in the minimum extent of scattering.

The above model can be extended to other similar solid solution systems which are oxygen ion conductors. However, this model does not hold good when compound formation occurs. Rigorous calculations of the potential energy of the oxygen ions as a function of position in the lattice will be necessary for a complete and accurate description of the conduction mechanism.

7 Conclusions

Solid solutions in the ternary system ZrO_2–CeO_2–Y_2O_3 have cubic fluorite structure throughout the composition range. Results of oxygen ion transport number measurements coupled with electrical conductivity data indicate that oxygen ions are the predominant current carriers at temperatures <1600 K and ambient oxygen partial pressure.

The isothermal variation of electrical conductivity with composition, x, exhibits a minimum around $x=0{\cdot}5$. The corresponding variation in activation energy follows the reverse trend, the maximum occurring at $x=0{\cdot}5$. This behaviour has been explained in terms of a simple model, according to which the changes in conductivity and activation energy are due to the varying degree of scattering of the mobile oxygen ions.

The electrical conductivity data, especially those for the high-ceria solid solutions, suggest that these materials can be used as hot electrodes in long-duration MHD channels.

References

1. Rosing, B. R. & Bowen, H. K., Materials for open cycle magnetohydrodynamic (MHD) channel. In *Critical Materials Problems in Energy Production*, ed. Charles Stein. Academic Press, New York, 1976, p. 335.
2. Markin, T. L., Bones, R. J. & Dell, R. M., High temperature solid electrolyte fuel cells. In *Superionic Conductors*, eds. C. D. Malwn & W. L. Roth. Plenum, New York, 1976, p. 15.
3. Rohatgi, V. K. & Venkatramani, N., Recent advances in MHD power generation, B.A.R.C. Technical Report, Bombay, 1981.
4. Rosing, B. R., Cadoff, L. H. & Gupta, T. K., *Proc. 6th Int. Conf. MHD Electrical Power Generation*, Washington, DC, 1975, p. 105.
5. Kroger, F. A. & Vink, H. J., Relations between the concentrations of imperfections in crystalline solids.. In *Solid State Physics*, ed. F. Seitz & D. Turnbull. Academic Press, New York, 1956, pp. 307–435.
6. Negas, T., Roth, R. S., McDaniel, C. L., Parker, H. S. & Oslon, C. D., Influence of K_2O on the cerium oxide–ZrO_2 system. *Proc. 12th Rare Earth Conf.*, CO, Vol. 2, ed. C. E. Lundin. University of Denver, Denver Research Institute, Denver, CO, 1976, p. 605.
7. Cales, B. & Baumard, J. F., Electrical properties of the ternary solid solutions $(ZrO_{2-x}$–$CeO_2)_9$–Y_2O_3. *Rev. Int. Hautes Temp. Refract., Fr.*, **17** (1980) 137.
8. Rao, C. N. R. & Subba Rao, G. V., Transition metal oxides. NSRDS-NBS 49, US Dept of Commerce/NBS, 1974.
9. Ananthapadmanabhan, P. V., Investigations on materials for MHD generator. PhD Thesis, University of Bombay, 1987.
10. Browell, K. W. & Doremus, R. H., Synthesis and evaluation of doped Y_2O_3 stabilised ZrO_2 for the production of hydrogen. *J. Am. Ceram. Soc.*, **60** (1977) 262.
11. Shannon, R. D. & Previtt, C. T., Effective ionic radii in oxides and fluorides. *Acta Cryst.*, B, **25** (1969) 955.
12. Azaroff, L. V., *Introduction to Solids*. McGraw-Hill, London, 1960.